

# Centrality dependence of strangeness and (anti)hyperon production at BNL RHIC

Jean Letessier

*Laboratoire de Physique Théorique et Hautes Energies  
Université Paris 7, 2 place Jussieu, F-75251 Cedex 05*

Johann Rafelski

*Department of Physics, University of Arizona, Tucson, Arizona, 85721, USA*

(Dated: June 14, 2005)

We evaluate strangeness produced in Au-Au interactions at  $\sqrt{s_{NN}} = 200$  GeV, as function of reaction participant number  $A$ , and obtain the relative strange quark content at hadronization. Strange baryon and antibaryon rapidity density yields are studied, relative to, and as function of, participant number, and produced hadron yields.

PACS numbers: 25.75.Nq, 24.10.Pa, 12.38.Mh

The experiments at the Relativistic Heavy Ion Collider (RHIC) study the properties of quark-gluon plasma (QGP) matter, a state that was present in the early Universe. We explore in this paper the production of baryons and antibaryons containing one or more strange quarks. Strange antibaryons offer a unique signature of the presence of QGP [1]. Their yields probe how QGP turns into conventional matter (hadronization).

At origin of this strange (anti)baryon signature is the high abundance of strangeness expected in QGP, combined with the high matter density at hadronization of this entropy rich phase [2]. A relatively small conventional production background enhances the importance of (multi)strange antibaryon QGP signature [3]. We use results of an analysis of the general pattern of particle production at central rapidity as function of  $A$  [4] for RHIC  $\sqrt{s_{NN}} = 200$  GeV Au-Au reactions. These results were obtained within the statistical hadronization model [5] (SHM) description of the PHENIX experimental central rapidity yields [6]  $dN_i/dy$ ,  $N_i = \pi^\pm, K^\pm, p$  and  $\bar{p}$  along with STAR experiment relative yields  $K^*(892)/K^-$  [7] and  $\phi/K^-$  [8].

The hadronization conditions for strangeness are presented for the first time here and will be used to predict the centrality dependent yields of strange and multi-strange baryons and antibaryons. These results are obtained without any adjustment or revision of Ref. [4]. The statistical model parameters allowing us to differentiate the degree of chemical equilibration is the phase space occupancy  $\gamma_i$ .  $\gamma_i$  has for each flavor ‘ $i$ ’ of quarks a similar role as the “blackness” of a gray-body photon-emitter: for  $\gamma < 1$  there are fewer particles than expected from a black-body source, and for  $\gamma > 1$  more. The SHM analysis of the final state hadron yields presumes thermal equilibrium, and we consider all chemical (non-)equilibrium conditions studied in literature:

1) Chemical non-equilibrium of valence light and strange quark pair abundance; this we expect to arise in a rapid transformation of the deconfined quark-matter into free-streaming hadrons. In such a sudden hadronization, there is no time to re-equilibrate the final state yields determined by fragmentation and recombination

of available QGP partons. Because the (chemically equilibrated) phase space in QGP, in general, has a different density compared to the hadronic gas (HG), QGP chemical equilibrium described by quark-matter space occupancies  $\gamma_s^Q = 1$ ,  $\gamma_q^Q = 1$  implies hadron chemical non-equilibrium, with the parameters  $\gamma_s^H \neq 1$ ,  $\gamma_q^H \neq 1$ .

2) Chemical semi-equilibrium, which may arise for sufficiently slow hadronization, allowing to re-equilibrate the light quark abundances after hadron formation,  $\gamma_q^H \rightarrow 1$ . Since strangeness re-equilibration is a considerably slower reaction process [9], it did not have sufficient time to develop. Alternatively, this chemical semi-equilibrium can also arise in reactions not involving a phase change, with particle production in hadron sector evolving to chemical equilibrium for non-strange hadrons, but strange hadrons not having enough time to reach the strangeness yield ‘absolute’ chemical equilibrium.

3) Full chemical equilibrium,  $\gamma_s^H = \gamma_q^H = 1$ , requires a complete re-equilibration, or, if there is no phase change, equilibration of all types of hadronic particles.

We assess the viability of QGP strange (anti)baryon signatures of deconfinement by comparing these three scenarios as function of  $A$ . For very peripheral collisions, also studied in Ref. [4], there was a significant deviation from chemical equilibrium with the strangeness yield being significantly reduced, as measured both, by quark occupancy  $\gamma_s^H/\gamma_q^H < 1$ , and the (nearly conserved) strangeness to entropy ratio  $s/S \simeq 0.019$ . Moreover, in this limit, the data fit employing chemical equilibrium  $\gamma_s^H = \gamma_q^H = 1$  did not yield a confidence level  $P[\%]$  comparable to the chemical non-equilibrium approach. The present analysis includes all results for  $A > 20$  which yield  $P[\%] > 60\%$ . With increasing  $A$ , for the chemical non-equilibrium statistical hadronization model, the strangeness occupancy  $\gamma_s^H$  was rising rapidly, reaching for most central collisions the value  $\gamma_s^H = 2.4$ . The relative yield of strangeness per entropy was found for the most central collisions,  $A \simeq 350$ , at  $s/S \simeq 0.028 \pm 0.002$ , which corresponds to the expectations one has for nearly chemically equilibrated QGP.

We show, in the top panel of Fig.1, the average strangeness density of the hadron source at central ra-

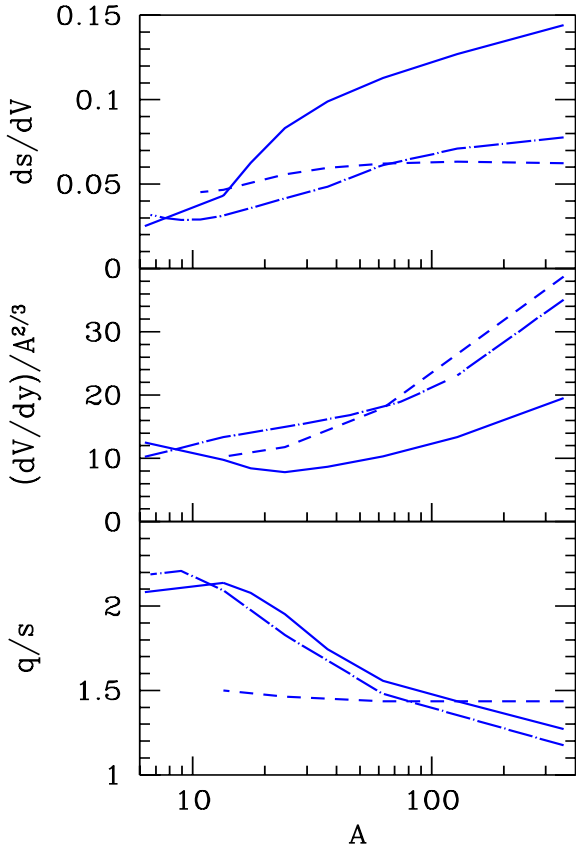


FIG. 1: Top panel: Strangeness density  $ds/dV$  [ $\text{fm}^{-3}$ ]; middle panel: geometrically reduced hadronization volume  $dV/dy/A^{2/3}$  [ $\text{fm}^{-3}$ ]; and bottom panel: the ratio of light quark to strange quark density  $q/s$  as function of  $A$ . Solid lines: chemical non-equilibrium; chain lines: chemical semi-equilibrium; and dashed lines: chemical equilibrium.

pidity, as function of  $A$ , at the time of hadronization:  $(ds/dy)/(dV/dy) = ds/dV = d\bar{s}/dV$ . For very peripheral collision systems, the central rapidity density is at  $ds/dV = 0.03/\text{fm}^3$ . As  $A$  increases, there is a significant increase in the strangeness density at hadronization in the chemical non-equilibrium model, with the full non-equilibrium (solid line) approaching a five-fold increase.  $ds/dV$  doubles in the semi-equilibrium case (chain line) and increases by 50% in chemical equilibrium model (dashed line).

This result combines two multiplicative factors:

- 1) The strangeness yield per unit of rapidity,  $ds/dy$ , which, in principle, can be directly estimated from the experimental yields of particles which were fitted, and is thus model independent.
- 2) The statistical volume per rapidity  $dV/dy$ , which is a model dependent result of the fit to the global particle yield pattern.

We show its behavior in the middle panel of Fig. 1, reduced by the initial state geometric scale factor  $A^{2/3}$ . For small  $A$ , the chemical non-equilibrium result shows a 40% reduction of the residual volume with increasing  $A$ , as would be expected for an increasing stopping power, *e.g.*, due to the progressive onset of deconfinement.

All models show, for large  $A$ , an increase of  $(dV/dy)/A^{2/3}$  with  $A$ , which can be interpreted as being due to the greater dynamic expansion prior to hadronization of the larger, initially more compressed system. For the chemical non-equilibrium model,  $(dV/dy)/A^{2/3}$  increases by 180% compared to minimum near  $A = 25$ . The yet larger increases, by a factor 3.5–4, seen for the chemical semi-equilibrium and equilibrium models, compensate for the chemical non-equilibrium factor  $\gamma_q^H \simeq 1.6$ . Some may consider such an increase excessive, in which case the result is an indirect evidence for  $\gamma_q^H > 1$ .

In order to gauge the impact of the strangeness hadronization density increase, we have to compare it to light quark density. as this effectively eliminated the model dependence. To obtain such a  $q/s$  ratio, we estimate the light quarks number, including any originating in hadronization fragmentation, from the final state entropy content. For quarks with thermal mass  $m_q \simeq 2T$ , for the classical massive gas the entropy per particle is  $S/N \simeq 5$ . Thus:

$$\frac{q}{s} \simeq \frac{1}{ds/dy} \left[ \frac{1}{k(S/N)} \left( \frac{dS}{dy} - k_s \frac{S}{N} \frac{ds}{dy} \right) \right]. \quad (1)$$

We reduced the total entropy content by the two ( $k_s = 2$ ) fractions  $s$  and  $\bar{s}$ , and divided by  $k(S/N) = 20$  to obtain the approximate average yield of the  $k = 4$  components  $q = u, \bar{u}, d$  and  $\bar{d}$ .

The chemical non-equilibrium  $q/s$  (solid line in bottom panel of Fig. 1) and semi-equilibrium (chain line) ratios  $q/s$  are identical within the error margin of this estimate. Strangeness is, at small  $A$ , suppressed by more than factor 2. For  $A \rightarrow 350$ , a 20% excess of light quark number compared to strange quark number remains. This can be understood, *e.g.*, as being due to the thermal strange quark mass being slightly larger than the light quark thermal mass, and both light and strange quarks approaching chemical equilibrium yields in the QGP. The hadron-phase chemical equilibrium result (dashed line) shows no variation with  $A$ . The increased yield of strangeness is consistent with the rise of the reduced reaction volume, which is implying an increase in the lifespan of the dense phase.

In the following, we discuss results which include decay products of weak decays: we count all pions from  $K_S$  decay, we include 10%  $K_L$  decay products, and all hyperon decay, *i.e.*, both pions and baryons are accepted. In particular, we included in our  $d\Lambda/dy$  and  $d\bar{\Lambda}/dy$ , all weak decays of  $d\Xi^-/dy$ ,  $d\bar{\Xi}^+/dy$  and  $d\Omega^-/dy$ ,  $d\bar{\Omega}^+/dy$ . These idealized assumptions will cause minor calculable correction for more realistic experimental acceptances. The interested reader can use the SHM implementation [5] to obtain results for other weak decay conditions.

We present, in Fig. 2, the predicted production rate of  $d\Lambda/dy$ ,  $d\bar{\Lambda}/dy$  (top panel),  $d\Xi^-/dy$ ,  $d\bar{\Xi}^+/dy$  (bottom panel) as function of  $dh^-/dy$  and  $d\pi^-/dy$  at central rapidity. The dependence on  $h^-$  is indicated in top, and on  $\pi^-$  in bottom of the figure. We note that the equilibrium model (dashed lines) predicts fewer (anti)hyperons.

We omitted the chemical semi-equilibrium lines which are in-between the two other models. The available experimental results shown are for  $\sqrt{s_{\text{NN}}} = 130$  GeV Au–Au rather than here considered 200 GeV reactions,  $d\Lambda/dy$ ,  $d\bar{\Lambda}/dy$  [10], and  $d\Xi^-/dy$ ,  $d\bar{\Xi}^+/dy$  [11]. Considering that at  $\sqrt{s_{\text{NN}}} = 200$  GeV the yields should be higher, the chemical nonequilibrium model is more likely to be consistent with the 200 GeV data.

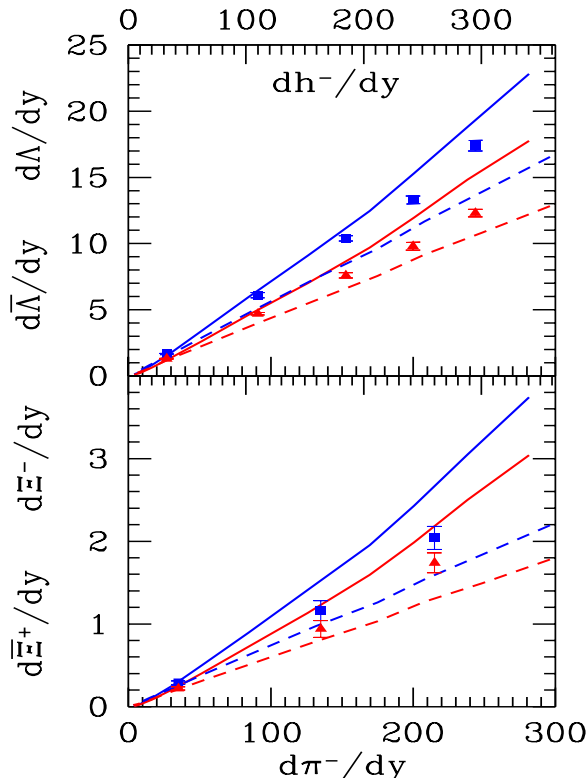


FIG. 2: (color online) The predicted hyperon (blue) and, in same panel directly below, antihyperon (red) yields. The rapidity yields are shown as function of both  $d\pi^-/dy$  (bottom scale) and  $dh^-/dy$  (top scale) for  $\sqrt{s_{\text{NN}}} = 200$  GeV Au–Au reactions. Solid lines for chemical non-equilibrium, and dashed lines for the chemical equilibrium. The experimental results (square symbols for hyperons and triangles for antihyperons) are from  $\sqrt{s_{\text{NN}}} = 130$  GeV Au–Au reactions, presented here for reader orientation.

We now turn to discuss the enhancement effect in production of hyperons and antihyperons. A way to study this enhancement is to consider the yield of the particle per hadron and/or per pion as function of hadron/pion yield. We present, in Fig. 3, the full set of hyperon theoretical predictions normalizing these with the  $\pi^-$  yield. We see that the normalized chemical equilibrium yield is flat, while the chemical non-equilibrium yields predict enhancement with  $A$ . This effect can be seen, in Fig. 2, as a slight up-bend in the particle yield at high  $A$ .

Such an up-bend is visible in the experimental  $\Lambda$  and  $\bar{\Lambda}$  results for  $\sqrt{s_{\text{NN}}} = 130$  GeV Au–Au reactions [10], however the data was not analyzed to reveal this effect. Considering result shown in Fig. 3, we suggest that a fit to

the experimental centrality dependence should be made allowing for a non-linear shape, *e.g.*:

$$dN/dy = a_1 h^- + 0.5a_2 (h^-)^2, \quad (2)$$

where predicted  $a_2$  is, up to a factor  $h^-/\pi^- = 1.2$ , the slope seen in Fig. 3, solid line.

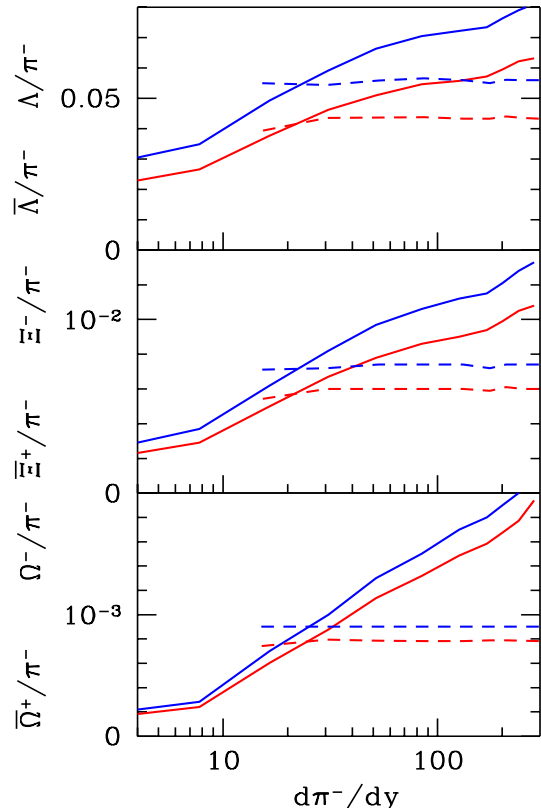


FIG. 3: (color online) The yields of hyperons (blue) and antihyperons (red),  $\Lambda$ ,  $\bar{\Lambda}$  (top panel),  $\Xi^-$ ,  $\bar{\Xi}^+$  (middle panel), and  $\Omega^-$ ,  $\bar{\Omega}^+$  bottom normalized with  $\pi^-$  yield, as function of  $d\pi^-/dy$ . The lines are as in Fig. 2.

Should  $a_2 \rightarrow 0$ , this would constitute reliable evidence for validity of the chemical equilibrium model: such a result relates closely to the flat  $q/s$  relative yield, in Fig. 1, bottom panel.  $a_2 \rightarrow 0$  means that there is no centrality dependence in relative strange and light quark abundances, and densities, at hadronization. This is expected for chemical equilibrium, but would require an extraordinary coincidence to occur at several centralities for chemical non-equilibrium. Therefore, this is a test for chemical equilibrium, more appropriate than the more common study of  $\gamma_s^H \rightarrow 1$  and  $\gamma_q^H \rightarrow 1$ . In the latter case, the fitted value of  $\gamma_{s,q}^H$  can be different from unity, due to incompleteness of the SHM set of hadron states.

There is another way to study enhanced production of strange hyperons [12]: we consider the hyperon yield normalized by  $A$ , as function of  $A$ . To obtain enhancement, we divide by the background signal defined to be the experimental yield for the smallest available system,

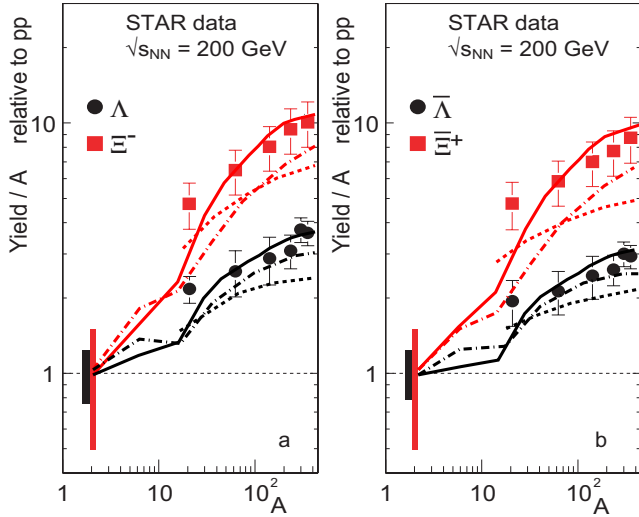


FIG. 4: (color online)  $\sqrt{s_{NN}} = 200$  GeV yields of hyperons  $d\Lambda/dy$  and  $d\Xi^-/dy$ , on left, and antihyperons  $d\bar{\Lambda}/dy$  and  $d\bar{\Xi}^+/dy$ , on right, normalized with, and as function of,  $A$ , relative to these yields in  $pp$  reactions. The lines are as in Fig. 2.

*e.g.*,  $A = 2$ . The STAR collaboration has stated the central rapidity yield of  $d\Lambda/dy$ ,  $d\bar{\Lambda}/dy$ ,  $d\Xi^-/dy$  and  $d\bar{\Xi}^+/dy$ , at  $\sqrt{s_{NN}} = 200$  GeV in this way, see Fig. 4 [13]. The experimental reduced yields vary for large  $A$ , with  $A$ . This behavior cannot be due to a reinterpretation of the enhancement as being due to the  $pp$  yield suppression, for it occurs at relatively large  $A$ .

We overlay, over these data, the *unsmoothed* results we obtained with SHM. To normalize the SHM predictions, we use the central values of  $pp$  yields stated in Ref. [14]:  $d(\Lambda + \bar{\Lambda})/dy = 0.066 \pm 0.006$ ,  $d(\Xi^- + \bar{\Xi}^+)/dy = 0.0036 \pm 0.0012$ ,  $\bar{\Lambda}/\Lambda = 0.88 \pm 0.09$  and  $\bar{\Xi}^+/\Xi^- = 0.90 \pm 0.09$ . Thus, we also extend the lines from  $A = 6.3$ , the smallest value considered in peripheral Au–Au interactions, to  $A = 2$ , where they assume by definition the value unity. Since the chemical equilibrium SHM fit is not valid below  $A = 20$  we do not continue this line. The edge, near to  $A = 20$ , is signaling the change in behavior of the SHM fit

associated with a possible phase change [4, 15].

The agreement of the chemical non-equilibrium result with all four data sets is remarkable. The reader should note that the relative yields and  $A$ -dependence of the  $\Lambda, \bar{\Lambda}, \Xi, \bar{\Xi}$  are correctly described by SHM model parameters derived from study of other particles. This is a remarkable accomplishment of the SHM. This remark applies to all three models considered, considering the magnitude of the normalization uncertainty, indicated at  $A = 2$ , in Fig. 4 — here we note that we cannot with required precision extract the absolute yields from Fig. 4 [13], and enter these in Fig. 3, considering the double logarithmic representation.

In this paper, we have explored the strangeness content of the RHIC fireball at its hadronization point found in Ref. [4]. We showed, as function of  $A$ , the behavior of the relative pre-hadron formation yields of light and strange quarks. Within the context of chemical non-equilibrium, the strangeness content increases rapidly with  $A$ . The reaction volume scales with  $A^{2/3}$ , however, the residual variation is characteristic of phase properties and expansion dynamics.

The increase in  $s/q$  with  $A$ , Fig. 1, is imaged in the rise of the specific per hadron yields of strange antibaryons, Fig. 3, with centrality. The variation of the strangeness yield with the reaction volume (impact parameter) is furthermore the source of the rapid rise of multi-strange (anti)baryon yield enhancement seen in Fig. 4.

The absolute strange (anti)baryon rapidity yields, Fig. 2, predicted for  $\sqrt{s_{NN}} = 200$  GeV, distinguish the hadronization models: the yields of  $d\Xi^-/dy$  and  $d\bar{\Xi}^+/dy$  are, for the chemical non-equilibrium case, 80% above those expected in the chemical equilibrium approach. The high experimental hyperon yields reported at  $\sqrt{s_{NN}} = 130$  GeV favor the chemical non-equilibrium hadronization. Future experimental results can as we have shown provide decisive distinction between the hadronization pictures considered.

Work supported by a grant from: the U.S. Department of Energy DE-FG02-04ER4131. LPTHE, Univ. Paris 6 et 7 is: Unité mixte de Recherche du CNRS, UMR7589.

- 
- [1] J. Rafelski and J. Letessier, Phys. Lett. B **469**, 12 (1999).  
J. Rafelski, Phys. Rep. **88**, 331 (1982), and references therein.
  - [2] J. Letessier, A. Tounsi, U. Heinz, J. Sollfrank and J. Rafelski, Phys. Rev. Lett. **70**, 3530 (1993).
  - [3] H. Weber, E. L. Bratkovskaya, W. Cassing and H. Stöcker, Phys. Rev. C **67**, 014904 (2003).
  - [4] J. Rafelski, J. Letessier and G. Torrieri, “Centrality dependence of bulk fireball properties at RHIC”, Physical Review C, (2005) in press, arXiv:nucl-th/0412072.
  - [5] G. Torrieri, W. Broniowski, W. Florkowski, J. Letessier and J. Rafelski, Comp. Phys. Com. **167**, 229 (2005), see: [www.physics.arizona.edu/~torrieri/SHARE/share.html](http://www.physics.arizona.edu/~torrieri/SHARE/share.html)
  - [6] S. S. Adler *et al.* [PHENIX], Phys. Rev. C **69**, 034909 (2004).
  - [7] J. Adams [STAR], Phys. Rev. C **71**, 064902 (2005).
  - [8] J. Adams *et al.* [STAR], Phys. Lett. B **612**, 181 (2005).
  - [9] P. Koch, B. Müller and J. Rafelski, Phys. Rept. **142**, 167 (1986).
  - [10] C. Adler *et al.* [STAR], Phys. Rev. Lett. **89**, 092301 (2002).
  - [11] J. Adams *et al.* [STAR], Phys. Rev. Lett. **92**, 182301 (2004).
  - [12] E. Andersen *et al.* [WA97], Phys. Lett. B **449**, 401 (1999).
  - [13] H. Caines [STAR], J. Phys. G **31**, S1057 (2005).
  - [14] M. Heinz [STAR], J. Phys. G **31**, S1011 (2005).
  - [15] J. Letessier and J. Rafelski, “Hadron production and phase changes in relativistic heavy ion collisions”, arXiv:nucl-th/0504028.